

## Supplementary Information

# **Formation of self-limited, stable and conductive interfaces between garnet electrolytes and lithium anodes for reversible lithium cycling in solid-state batteries**

*Minghui He, Zhonghui Cui,<sup>\*</sup> Cheng Chen, Yiqiu Li, and Xiangxin Guo<sup>\*</sup>*

<sup>a</sup>. State Key Laboratory of High Performance Ceramics and Superfine Microstructure, Shanghai Institute of Ceramics, Chinese Academy of Sciences, Shanghai 200050, China.

\*E-mail: [zhonghui.cui@gmail.com](mailto:zhonghui.cui@gmail.com) (Z. Cui) or [xxguo@mail.sic.ac.cn](mailto:xxguo@mail.sic.ac.cn) (X. Guo)

<sup>b</sup>. University of Chinese Academy of Sciences, Beijing 100039, China

<sup>c</sup>. College of Physics, Qingdao University, Qingdao 266071, China

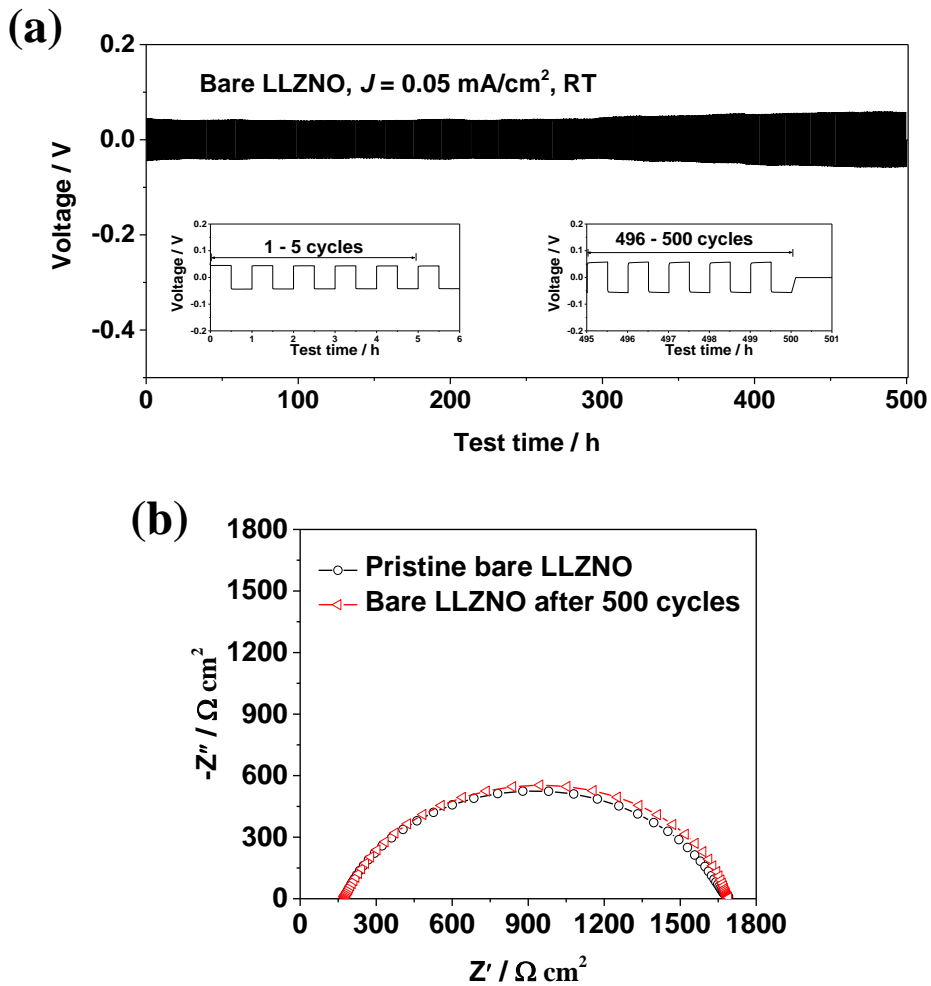


**Figure S1** **(a)** Voltage profile of the Li plating/stripping for the Li/garnet/Li symmetric cells with bare LLZNO electrolyte at a current density of  $0.05 \text{ mA cm}^{-2}$  under RT. The voltage shows perfect plateaus through the whole testing process that suggests the symmetric cell Li/LLZNO/Li cycles stable for over 500 h at a low current density. **(b)** Comparison of the EIS profiles of Li/LLZNO/Li symmetric cell before and after the test of **(a)**. The good performance of the symmetrical cell mainly due to the stability and high density of the electrolyte pellet, which are beneficial for suppressing the dendrite at a low current density.<sup>1-3</sup>

**Table S1.** Stability of Nb-containing garnet-type electrolytes versus Li metal in literatures.

Solid-state electrolyte (SSE)	cell structure	temperature	stability	reference
$\text{Li}_7\text{La}_{2.75}\text{Ca}_{0.25}\text{Zr}_{1.75}\text{Nb}_{0.25}\text{O}_{12}$	$\text{Li/SSE/Li}_2\text{FeMn}_3\text{O}_8$	RT	Y	4
$\text{Li}_{6.85}\text{La}_{2.9}\text{Ca}_{0.1}\text{Zr}_{1.75}\text{Nb}_{0.25}\text{O}_{12}$	$\text{Li/Si coated SSE/Li}$	RT	Y	5
$\text{Li}_{6.5}\text{La}_3\text{Zr}_{1.5}\text{Nb}_{0.5}\text{O}_{12}$	$\text{Li/SSE/Li}$	$23.5 \pm 1^\circ\text{C}$	N	6
$\text{Li}_{6.25}\text{La}_3\text{Nb}_{0.75}\text{Zr}_{1.25}\text{O}_{12}$	$\text{Li/SSE/Li}$	RT	N	7
$\text{Li}_{6.25}\text{La}_3\text{Nb}_{1.375}\text{Sc}_{0.625}\text{O}_{12}$	$\text{Li/SSE/Li}$	RT	N	7
$\text{Li}_{6.75}\text{La}_3\text{Zr}_{1.75}\text{Nb}_{0.25}\text{O}_{12}$	$\text{Li/SSE/LiCoO}_2$	$25^\circ\text{C}$	Y	8
$\text{Li}_{6.8}(\text{La}_{2.95},\text{Ca}_{0.05})(\text{Zr}_{1.75},\text{Nb}_{0.25})\text{O}_{12}$	$\text{Li/SSE/LiCoO}_2$	$25^\circ\text{C}$	Y	9
$\text{Li}_{6.75}\text{La}_3\text{Zr}_{1.75}\text{Nb}_{0.25}\text{O}_{12}$	$\text{Li/SSE/LiCoO}_2$	$25^\circ\text{C}$	Y	10
$\text{Li}_{6.75-x}\text{La}_3\text{Zr}_{1.75}\text{Nb}_{0.25}\text{O}_{12-0.5x}$	$\text{Li/SSE/Li}$	$25^\circ\text{C}$	Y	11
$\text{Li}_{6.85}\text{La}_{2.9}\text{Ca}_{0.1}\text{Zr}_{1.75}\text{Nb}_{0.25}\text{O}_{12}$	$\text{Li/SSE/LiFePO}_4$	RT	Y	12
$\text{Li}_{6.375}\text{La}_3\text{Zr}_{1.375}\text{Nb}_{0.625}\text{O}_{12}$	$\text{Li/SSE/Li}$	RT	Y	This work

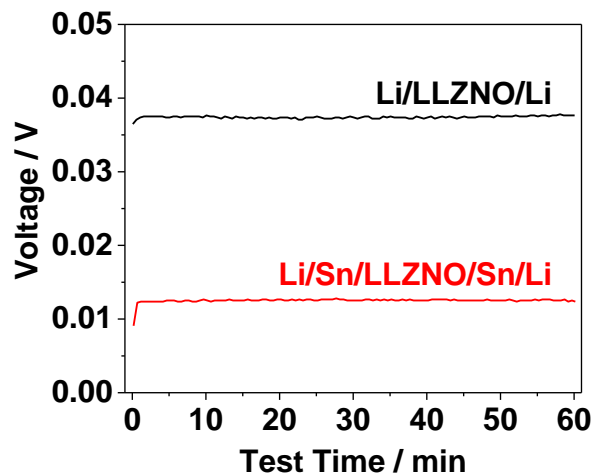


**Figure S2.** The direct current (DC) polarization of the symmetric cell using the LLZNO electrolyte with or without Sn thin-film modification. The cell with bare LLZNO electrolyte shows a voltage of 0.037 V, which is about 3 times larger than that of the cell with Sn thin-film modified LLZNO electrolyte.

**Table S2** Comparison of the interfacial resistance of Li/garnet with and without Sn thin-film obtained from EIS and DC polarization.

Interface	Resistance obtained from	
	EIS	DC polarization
Li/LLZNO	$758 \Omega \text{ cm}^2$	$750 \Omega \text{ cm}^2$
Li/Sn-LLZNO	$46.6 \Omega \text{ cm}^2$	$39 \Omega \text{ cm}^2$



**Figure S3.** The photo of a bare LLZNO pellet having suffered the formation of lithium dendrite after cycling at a current density of  $0.5 \text{ mA cm}^{-2}$  under RT. This serious consequence indicates that the contact and wetting performance between garnet and lithium is one of the principle hurdles hindering the development of SSBs.

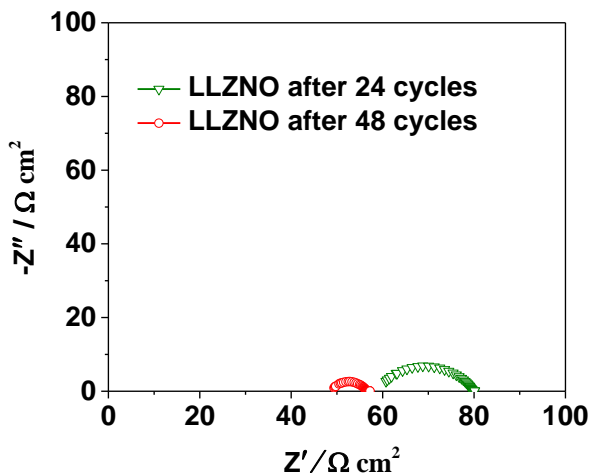


**Figure S4.** EIS profiles of a symmetric cell using bare garnet with Li electrodes. This indicates the formation of Li dendrite and then cell shortcut caused by the dendrite penetration (as shown in **Figure S3**).

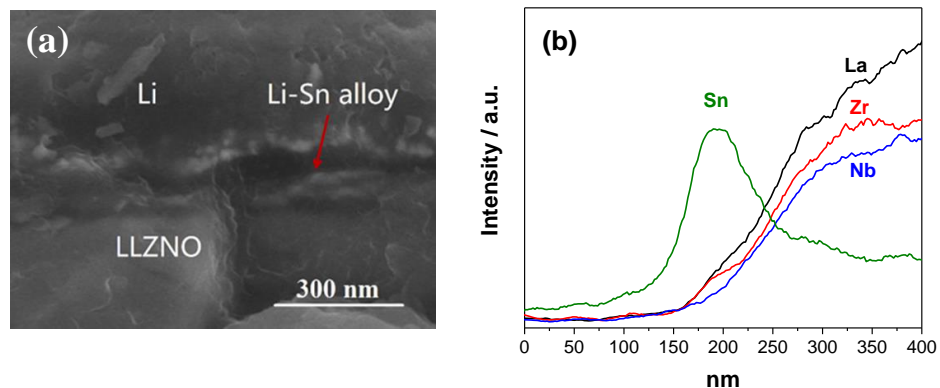


**Figure S5.** (a) The cross-section SEM and (b) EDX line scanning profile of the symmetric cell using Sn thin-film modified LLZNO, which confirms the lithium are tightly adhered to the LLZNO electrolyte even after 500 cycles through the bridge of Li-Sn alloy layer.

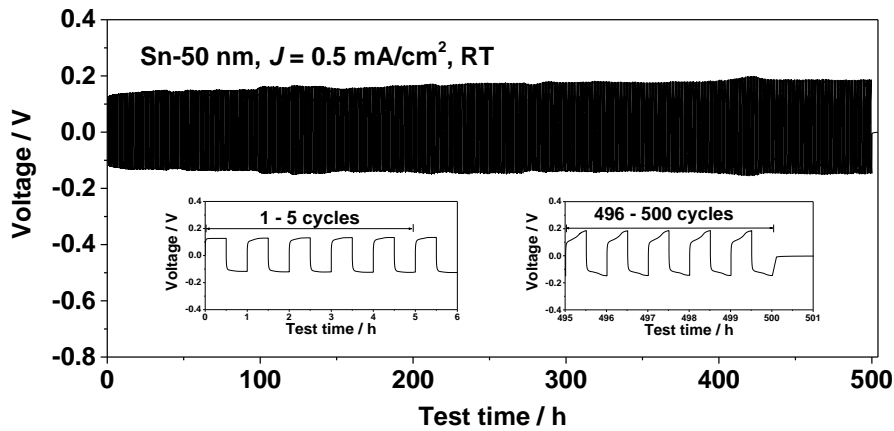


**Figure S6.** Voltage profile of the Li plating/stripping for the Li/garnet/Li symmetric cell with 50 nm Sn thin-film modified LLZNO electrolyte at a current density of 0.5 mA cm<sup>-2</sup>. Compared with the cell with 10 nm Sn thin-film modified LLZNO electrolyte, the voltage for lithium plating and stripping shows a slight increase to 0.13 V even at the first cycle and the voltage plateaus become irregular during the 500 cycles (insets). However, the cycling remains stable for over 500 cycles, clearly indicating the effectiveness on improving garnet-lithium interfacial performance by modifying the LLZNO electrolyte with Sn thin-film.

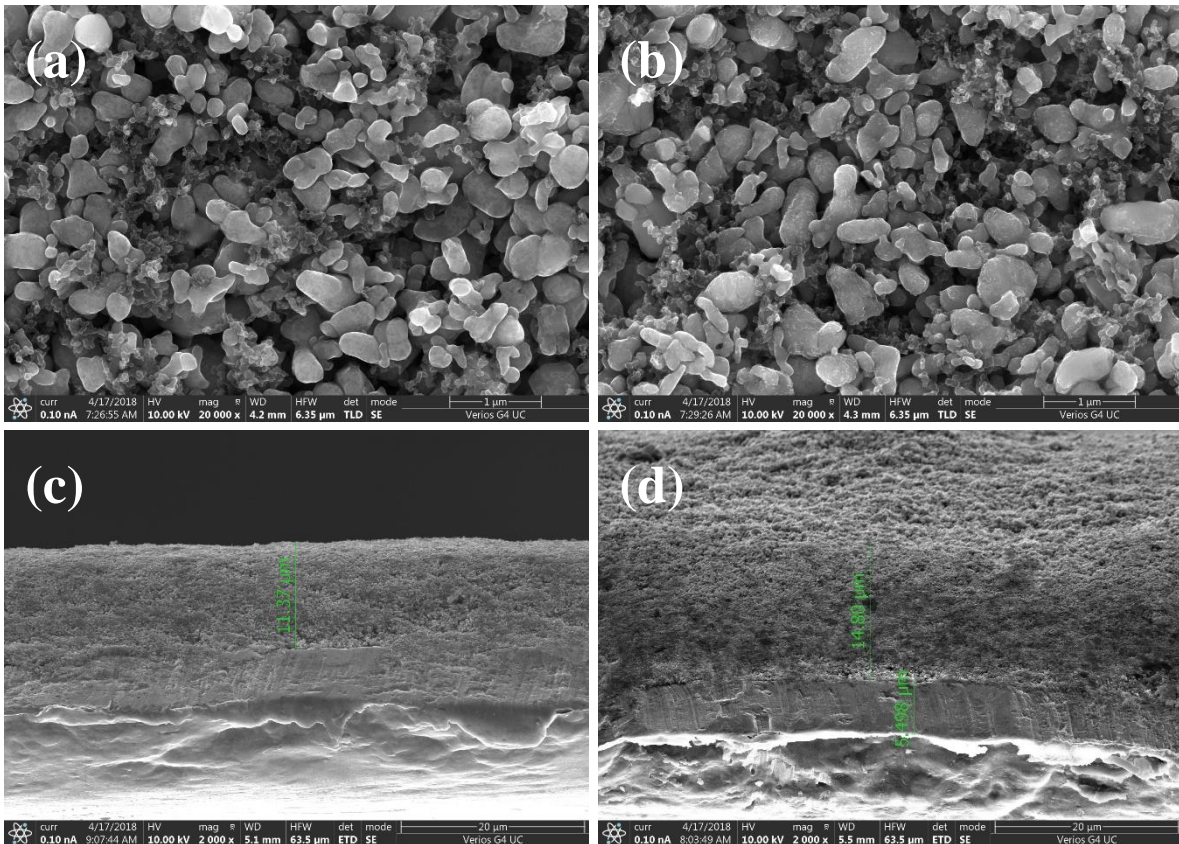


**Figure S7** The SEM images of the surface and cross-sectional of the LFP:C:PVDF composite cathode with Al foil current collector. The surface morphology before cycling **(a)** and after galvanostatic charging-discharging 100 cycles at 0.1 C **(b)** and the cross-section SEM before cycling **(c)** and after galvanostatic charging-discharging 100 cycles at 0.1 C **(d)**.

The brightly olive-shaped LiFePO<sub>4</sub> particles<sup>13</sup> with a size of around 1  $\mu\text{m}$  are evenly distributed in the cathode **(a)**. Worth noting that many interspaces appear between the large LiFePO<sub>4</sub> particles. The cross-section SEM indicates that the LiFePO<sub>4</sub> cathode has a thickness of  $\sim$ 11  $\mu\text{m}$  **(c)**. These features are well reserved as shown in **b** and **d**. Clearly, there is no visible change in microstructure before and after the electrochemical characterization, which contributes the stable cycling of Li/Sn-LLZNO/LiFePO<sub>4</sub> full cells.

## Reference:

1. R. Raj and J. Wolfenstine, *J. Power Sources*, 2017, **343**, 119-126.
2. C. L. Tsai, V. Roddatis, C. V. Chandran, Q. Ma, S. Uhlenbruck, M. Bram, P. Heitjans and O. Guillon, *ACS Appl. Mater. Inter.*, 2016, **8**, 10617-10626.
3. L. Cheng, W. Chen, M. Kunz, K. Persson, N. Tamura, G. Chen and M. Doeff, *ACS Appl. Mater. Inter.*, 2015, **7**, 2073-2081.
4. X. Han, Y. Gong, K. K. Fu, X. He, G. T. Hitz, J. Dai, A. Pearse, B. Liu, H. Wang, G. Rubloff, Y. Mo, V. Thangadurai, E. D. Wachsman and L. Hu, *Nat. Mater.*, 2017, **16**, 572-579.
5. W. Luo, Y. Gong, Y. Zhu, K. K. Fu, J. Dai, S. D. Lacey, C. Wang, B. Liu, X. Han, Y. Mo, E. D. Wachsman and L. Hu, *J Am Chem Soc*, 2016, **138**, 12258-12262.
6. Y. Kim, A. Yoo, R. Schmidt, A. Sharafi, H. Lee, J. Wolfenstine and J. Sakamoto, *Frontiers in Energy Research*, 2016, **4**.
7. H. Nemori, Y. Matsuda, S. Mitsuoka, M. Matsui, O. Yamamoto, Y. Takeda and N. Imanishi, *Solid State Ionics*, 2015, **282**, 7-12.
8. S. Ohta, T. Kobayashi, J. Seki and T. Asaoka, *J. Power Sources*, 2012, **202**, 332-335.
9. S. Ohta, J. Seki, Y. Yagi, Y. Kihira, T. Tani and T. Asaoka, *J. Power Sources*, 2014, **265**, 40-44.
10. S. Ohta, T. Kobayashi and T. Asaoka, *J. Power Sources*, 2011, **196**, 3342-3345.
11. K. Ishiguro, Y. Nakata, M. Matsui, I. Uechi, Y. Takeda, O. Yamamoto and N. Imanishi, *J. Electrochem. Soc.*, 2013, **160**, A1690-A1693.

12. W. Luo, Y. Gong, Y. Zhu, Y. Li, Y. Yao, Y. Zhang, K. K. Fu, G. Pastel, C.-F. Lin, Y. Mo, E. D. Wachsman and L. Hu, *Adv. Mater.*, 2017, **29**, 1606042.
13. F. Du, N. Zhao, Y. Li, C. Chen, Z. Liu and X. Guo, *J. Power Sources*, 2015, **300**, 24-28.